

1 **Identification of evolutionarily conserved virulence factor by selective pressure analysis**
2 **of *Streptococcus pneumoniae***

3

4 Masaya Yamaguchi^{a*}, Kana Goto^{a, b}, Yujiro Hirose^a, Yuka Yamaguchi^a, Tomoko Sumitomo^a,

5 Masanobu Nakata^a, Kazuhiko Nakano^b, Shigetada Kawabata^a

6

7 ^aDepartment of Oral and Molecular Microbiology, Osaka University Graduate School of

8 Dentistry, Suita, Osaka, Japan

9 ^bDepartment of Pediatric Dentistry, Osaka University Graduate School of Dentistry, Suita,

10 Osaka, Japan

11

12

13 *Address correspondence to Masaya Yamaguchi, yamaguchi@dent.osaka-u.ac.jp

14 **Running title:** Identification of virulence factor by evolutionary analysis

15 **Keywords:** *Streptococcus pneumoniae*, Evolutionary analysis, Choline-binding protein,

16 Evolutionary conservation

17 **Abstract**

18 Evolutionarily conserved virulence factors can be candidate therapeutic targets or vaccine
19 antigens. Here, we investigated the evolutionary selective pressures on 16 pneumococcal
20 choline-binding cell-surface proteins since *Streptococcus pneumoniae* is one of the pathogen
21 posing the greatest threats to human health. Phylogenetic and molecular analyses revealed
22 that *cbpJ* had the highest codon rates to total numbers of codons under significant negative
23 selection among those examined. Our *in vitro* and *in vivo* assays indicated that CbpJ
24 functions as a virulence factor in pneumococcal pneumonia by contributing to evasion of
25 neutrophil killing. Deficiency of *cbpL* under relaxed selective pressure also caused a similar
26 tendency but showed no significant difference in mouse intranasal infection. Thus, molecular
27 evolutionary analysis is a powerful tool that reveals the importance of virulence factors in
28 real-world infection and transmission, since calculations are performed based on bacterial
29 genome diversity following transmission of infection in an uncontrolled population.

30 Improper use of antibiotics creates evolutionary pressures that drive bacteria to acquire drug
31 resistance by natural mutation and/or horizontal transfer of resistance genes. This is a major
32 public health threat: it is estimated that drug-resistant infections cause 10 million deaths
33 annually and may result in economic losses reaching 100 trillion US dollars by 2050¹.
34 However, a target-to-hit screen typically requires approximately 24 discovery projects and 94
35 million US dollars, and the baseline total cost is 1.8 billion US dollars over 13 years to launch
36 a new drug². In fact, the number of new antibiotics developed and approved has steadily
37 decreased in the past three decades, leaving fewer options for treating resistant bacteria³.

38 *Streptococcus pneumoniae* is one of the pathogens posing the greatest threat to human
39 health^{4,5}. *S. pneumoniae* belongs to the mitis group^{6,7} and is a major cause of pneumonia,
40 sepsis, and meningitis^{8,9}. In 2015, pneumococcal pneumonia caused over 1.5 million deaths
41 in individuals of all ages, and this rate increased in people over 70 years old between 2005
42 and 2015¹⁰, which is especially problematic since the elderly population is growing in many
43 parts of the world. Although pneumococcal conjugate vaccines have considerable benefits,
44 non-vaccine pneumococcus serotypes have increased worldwide^{11,12}.

45 Conflict between the host immune system and pathogens leads to an evolutionary
46 arms races known as the “Red Queen” scenario^{13,14}. Protein regions at the host–pathogen

47 interface are subjected to the strongest selective pressure and thus evolve under positive
48 selection. Adaptive evolution has been reported in genes related to the mammalian immune
49 system such as pattern recognition receptors¹⁴. Concerning negative/purifying selection,
50 Jordan *et al.* compared two whole genome sequences and showed that essential bacterial
51 genes appear to demonstrate substantially lower average values of synonymous and
52 nonsynonymous nucleotide substitution rates compared to those in nonessential genes¹⁵.
53 However, to our knowledge, comprehensive evolutionary analysis on codons of genes
54 encoding bacterial cell surface proteins has not been performed. Mutations on essential genes
55 directly cause host death because essential genes encode proteins to maintain basic bacterial
56 survival such as central metabolism, DNA replication, translation of genes into proteins, and
57 so on. Meanwhile, nonessential genes are under negative/purifying selection, which is
58 important for the survival and/or success of the species in the host and/or the environment as
59 non-synonymous substitution of codons can lead to lineage extinction (Fig. 1). Phylogenetic
60 and molecular evolutionary analyses can reveal the number of codons under
61 negative/purifying selection in a species. Because alterations in amino acid residues in
62 regions under negative selective pressure are not allowed, drugs targeting these regions
63 would be less likely to promote the development of resistance through natural mutation.

64 We analysed pneumococcal choline-binding proteins (CBPs) localised on the bacterial
65 cell surface through interaction with choline-binding repeats and phosphoryl choline on the
66 cell wall. At least some CBPs play key roles in cell wall physiology, in pneumococcal
67 adhesion and invasion, and in evasion of host immunity. *S. pneumoniae* harbours various
68 CBPs including *N*-acetylmuramoyl L-alanine amidase (LytA), which induces
69 pneumococcal-specific autolysis¹⁶⁻¹⁸. Pneumococcal surface protein A (PspA) is a highly
70 variable protein and inhibits complement activation¹⁷⁻²⁰. Choline binding protein A (CbpA;
71 also called PspC) works as a major pneumococcal adhesin and contributes to evasion of host
72 immunity via interaction with several host proteins^{17,18,21}. Choline binding protein L (CbpL)
73 contains the choline binding repeats sandwiched between the Excalibur and lipoproteins
74 domains and works as an anti-phagocytic factor²². Although several CBPs have been
75 characterised, their phylogenetic relationships remain unclear and the unclassified gene
76 names are confusing. We first analysed the distribution of genes encoding CBPs based on
77 pneumococcal genome sequences. Orthologues of genes in each strain were identified by
78 phylogenetic analysis. We then calculated the evolutionary selective pressure on each codon
79 from the phylogenetic trees and aligned sequences. We found that *cbpJ* contains the highest
80 rate of codons under negative selection. CbpJ has no known functional domains except signal

81 sequences and choline-binding repeats, and its role in pneumococcal pathogenesis is unclear.

82 Functional analyses revealed that CbpJ contributes to evasion of host neutrophil-mediated

83 killing in pneumococcal pneumonia. Thus, evolutionary analysis focusing on negative

84 selection can reveal novel virulence factors.

85 **Results**

86 **Distribution of *cbp* genes among pneumococcal strains**

87 Genes encoding CBPs among pneumococcal strains were extracted by tBLASTn search
88 (Supplementary Table 1). Some genes were re-annotated since the search results showed that
89 certain homologous regions were not matched to annotated open reading frames (ORFs). In
90 strain SPNA45, *SPNA_01670* contains both predicted promoter regions and intact ORF
91 structures of *cbpF* and *cbpJ*. On the other hand, *cbpG*-homologous regions in strains R6, D39,
92 SPN034183, SPN994038, and SPN994039 did not contain promoters (Supplementary Table 1
93 and Supplementary Table 2). Orthologous relationships of each gene were analysed. The
94 distribution of *cbp* genes was not correspondent with capsular serotypes (Fig. 2A). Four
95 genes—i.e., *lytA*, *lytB*, *cbpD*, and *cbpE*—were conserved as intact ORFs in all 28
96 pneumococcal strains (Fig. 2A). Other *cbp* genes contained frameshift mutations in the
97 orthologues or were absent in some strains.

98

99 **Phylogenetic relationships in pneumococcal CBPs**

100 Phylogenetic relationships of genes encoding CBPs in pneumococcal species are confusing
101 since some genes in the same cluster show high similarity to each other. To clarify the

102 relationships, we compared common nucleotide sequences among genes encoding CBPs in
103 the strain TIGR4. Maximum likelihood and Bayesian phylogenetic analyses revealed two
104 common clusters: one comprising *cbpF*, *cbpG*, *cbpJ*, *cbpK*, and *cbpC*, and the other
105 comprising *lytA*, *lytB*, *lytC*, *cbpL*, and *cbpE* (Fig. 2B and Supplementary Fig. 1). The names
106 of some CBP genes were not consistent with those of phylogenetically related genes. In
107 particular, *cbpF*, *cbpG*, *cbpJ*, and *cbpK* were located close to each other in pneumococcal
108 genomes and showed high similarity. We thus defined orthologous genes in each
109 pneumococcal strain based on maximum likelihood and Bayesian phylogenetic analyses (Fig.
110 3 and Supplementary Fig. 2). The gene locus tag numbers in orthologous relationships are
111 shown in Supplementary Table 1. The sequence similarity of *cbpF*, *cbpG*, *cbpJ*, and *cbpK*
112 and their close proximity within genomes indicated that a common ancestral *S. pneumoniae*
113 acquired the genes by duplication. Phylogenetic trees showed well-separated clusters of each
114 gene. These independent relationships indicated that horizontal gene transfer did not
115 contribute to the spread of *cbpF*, *cbpG*, *cbpJ*, and *cbpK* in *S. pneumoniae* species, despite
116 their ability to take up exogenous DNA. The genetic diversity of these genes may have been
117 established by accumulation of natural mutations during pneumococcal transmission.
118

119 **Evolutionary selective pressures on each of the CBP codons**

120 To evaluate the significance of CBPs in real-life infection and transmission, we performed
121 molecular evolutionary calculations based on bacterial genome diversity established after
122 transmission of infection in an uncontrolled population. The nucleotide sequences of each
123 CBP were aligned by codon, and conserved common codons were used for phylogenetic
124 analysis (Supplementary Fig. 3). The selective pressure on each gene was calculated based on
125 the phylogenetic trees and aligned sequences (Table 1). The rates of codons under negative
126 selection are visualised in Supplementary Figure 4. Over 13% of total codons in *cbpJ* and
127 *lytA* were under negative selection compared to less than 5% for other *cbp* genes, indicating
128 that these genes play an important role in the success of *S. pneumoniae* species. On the other
129 hand, *pspA* encoding the genetically divergent virulence factor PspA, contained fewer
130 evolutionarily conserved codons, but had the highest numbers of codons under positive
131 pressure. Additionally, there were no evolutionarily conserved codons in *cbpG*, *cbpC*, and
132 *cbpL*. The latter two had no common codons as few genes had frameshift mutations. When
133 we re-calculated selective pressure without these genes, we found a low rate of codons under
134 negative selection among CBP-encoding genes (Supplementary Table 3).

135

136 **CbpJ acts as a virulence factor in pneumococcal pneumonia**

137 While CbpJ had the highest rate of codons under negative selection among pneumococcal
138 CBPs, it has no known functional domains except a choline-binding repeat in its amino acid
139 sequence. Moreover, its role in pneumococcal pathogenesis is unknown. In contrast, CbpL
140 had no common comparable codons and showed limited numbers of evolutionarily conserved
141 codons even after the above-described adjustment. The domain structures and codons of CbpJ
142 and CbpL under negative selection are shown in Figure 4A. The domains were searched
143 using MOTIF Libraries including PROSITE, NCBI-CDD, and P-fam²³⁻²⁶. To assess the roles
144 of CbpJ and CbpL in pneumococcal pathogenesis, we generated mutant strains deficient in
145 the corresponding genes. The mutant strains showed a slightly steeper growth curve in THY
146 medium (Supplementary Fig. 5A). There were no differences among the strains in minimum
147 inhibitory concentration (MIC) and minimum bactericidal concentration (MBC) values for
148 penicillin G, and bacterial morphology (Supplementary Table 4 and Supplementary Fig. 5B).
149 WT and mutant strains in stationary phase showed that most cells were stained violet,
150 whereas almost all cells of strains in the decline phase were stained pink probably due to
151 autolysis (Supplementary Fig. 5B). The *lytA* gene expression was slightly increased in the
152 $\Delta cbpJ$ strain compared to that in the WT strain at the log and decline phases (Supplementary

153 Fig. 5C). However, as described above, the difference did not seem to affect pneumococcal
154 autolysis substantially. We first performed a mouse intranasal infection assay to investigate
155 the role of CbpJ and CbpL in pneumonia. Mice intranasally infected with strain $\Delta cbpJ$
156 showed an improved survival rate compared to those infected with WT *S. pneumoniae*;
157 although a similar tendency was observed for $\Delta cbpL$ -infected relative to WT mice; the
158 difference was not statistically significant (Fig. 4B). The number of bacteria in the
159 bronchoalveolar lavage fluid (BALF) from $\Delta cbpJ$ -infected mice was lower than that in the
160 BALF from $\Delta cbpL$ - and WT-infected mice (Fig. 4C). We also performed competitive assay
161 by intranasal co-infection with the WT and $\Delta cbpJ$ strains. The BALF at 24 h after infection
162 showed fewer bacterial CFUs of $\Delta cbpJ$ compared to those of the WT (Fig. 4D). We also
163 examined whether CbpL or CbpJ contributes to the association of *S. pneumoniae* with
164 alveolar epithelial cells and found that WT *S. pneumoniae* as well as $\Delta cbpL$ and $\Delta cbpJ$
165 mutant strains did not differ in their ability to adhere to A549 human alveolar epithelial cells
166 (Fig. 4E).

167 However, the *S. pneumoniae* WT strain exhibited extensive inflammatory cell
168 infiltration and bleeding compared to that with the $\Delta cbpJ$ strain. Histological examination of
169 lung tissue from intranasally-infected mice showed that $\Delta cbpJ$ induced milder inflammation

170 compared to the WT strain. Lung tissue from $\Delta cbpL$ -infected mice showed moderate
171 inflammation (Fig. 5A). We also measured the bacterial survival rate after incubation with
172 human neutrophils in the absence of serum. Strains $\Delta cbpJ$ and $\Delta cbpL$ had a lower survival
173 rate than that of the WT, whereas $\Delta cbpJ$ showed a slightly increased growth rate compared to
174 that of the WT and $\Delta cbpL$ strains in RPMI 1640 medium without neutrophils (Fig. 5B and
175 Supplementary Fig. 5D). We also generated recombinant CbpJ using a codon-optimized *cbpJ*
176 sequence for expression in *E. coli* and measured the bacterial survival rate after incubation
177 with neutrophils and the recombinant protein. In the presence of recombinant CbpJ, the
178 survival rate of the $\Delta cbpJ$ strain was recovered (Supplementary Fig. 6). These results suggest
179 that CbpJ contributes to the evasion of neutrophil-mediated killing. Next, we performed a
180 mouse intravenous infection assay to investigate the role of CbpJ and CbpL in sepsis. In the
181 infection model, the survival rates of $\Delta cbpL$ - and $\Delta cbpJ$ -infected mice did not differ
182 significantly from those of mice infected with WT *S. pneumoniae* (Fig. 5C). We also
183 performed a blood bactericidal assay. The survival rates of $\Delta cbpJ$ and $\Delta cbpL$ strains in mouse
184 blood were comparable to those of the WT strain (Fig. 5D). We also found that incubation of
185 *S. pneumoniae* in human plasma for 3 h inhibited the expression of *cbpL* and *cbpJ*, as
186 determined by quantitative real-time (q)PCR (Fig. 5E). These results indicate that CbpJ acts

187 as a pneumococcal virulence factor in lung infection by contributing to the evasion of
188 neutrophil-mediated killing, whereas CbpJ has no role in bacterial survival in blood. In
189 addition, *cbpL* deficiency in strain TIGR4 did not significantly attenuate pathogenesis in the
190 mouse lung and blood infection.

191 **Discussion**

192 In this study, we investigated the evolutionarily conserved rates of CBP codons since these
193 cell surface proteins directly interact with the external environment, which induces rapid rates
194 of evolution in genes involved in genetic conflicts¹⁴. Evolutionary analysis based on
195 phylogenetic relationships can reveal regions in which the encoded amino acids are not
196 allowed to change even under selective pressure. The genetic diversity of *S. pneumoniae*
197 isolated from patients was the result of transmission in a real population. Thus, the
198 evolutionary conservation rate is a parameter that reflects the importance of the protein in
199 human infection. Although so-called arms races involve both the host and bacteria, most
200 studies on genetic diversity have focused on the former^{14,27-29}. For example, evolutionary
201 studies based on inter-species comparisons have shown that most of the positive selection
202 targets in host receptors are located in regions that are responsible for direct interactions with
203 pathogens. Our study focused on negative selection targets in bacterial surface proteins
204 through an evolutionary analysis based on intra-species comparisons. This approach enabled
205 us to estimate the contribution of bacterial proteins to species success throughout the life
206 cycle, including inside the host and during the transmission phase.

207 We previously detected bacterial virulence factors by function prediction – e.g., by

208 searching for conserved motifs/domains, constructing random transposon libraries, or
209 analysing the biochemical properties of the pathogen³⁰⁻³⁴. Although these laboratory-based
210 approaches are valuable, they are time-consuming and costly, and may not yield the expected
211 results. It is useful to examine the correlation between a target molecule and clinical features
212 as this can minimise the time and cost required for analysis. Furthermore, in basic studies on
213 bacterial pathogens, animal infection models are often used to determine whether a bacterial
214 molecule acts as a virulence factor. Although this is the best means of obtaining *in vivo*
215 information, it is unclear how accurately it reflects the clinical condition in humans.
216 Combining an evolutionary analysis and an animal model would thus be highly effective for
217 evaluating the functional significance of a putative virulence factor.

218 Genome-wide association study (GWAS) is a powerful tool for identifying the
219 relationship between genetic variants – mainly single nucleotide polymorphisms (SNPs) –
220 and phenotype, such as in diseases. As GWAS has become more prevalent, various programs
221 and software packages have been developed for this purpose^{35,36}. On the other hand, this
222 approach has certain limitations including the requirement for an appropriate control group
223 and detailed information regarding phenotype. In infectious diseases, it can be difficult to
224 quantify clinical features recorded at different medical centres. Furthermore, in the case of

225 most pathogens, there are no natural attenuated or avirulent strains that can serve as a control
226 group. Our evolutionary analysis has the advantage that it can be performed with genomic
227 information of pathogenic strains only by assuming the presence of pathogens as a phenotype
228 evading natural selection. Since synonymous and non-synonymous substitutions are
229 estimated to occur with equal probability under no selective pressure, a population in which
230 the latter has resulted in extinction by natural selection can serve as a control group. While
231 we have shown in the current study that evolutionary analysis with a small population has the
232 power to detect evolutionarily conserved proteins, a larger population would allow a
233 higher-resolution analysis, including detection of conserved regions in some pathogenic
234 strains isolated from a specific site of infection or pathological condition. Since this analysis
235 involves simultaneous processing of aligned nucleotide and amino acid sequences, more
236 information is obtained from only SNPs extracted from nucleotide sequences. In addition,
237 automated phylogenetic and evolutionary analyses are needed to analyse a large population.
238 Therefore, the development of software packages for meta-data is expected to aid the
239 widespread application of this analytical approach.

240 There are some limitations to our evolutionary analysis. Firstly, although it can detect
241 evolutionarily conserved proteins, it cannot identify diverse virulence factors such as PspA

242 and CbpA within species^{19,37,38}. Similarly, virulence factors recently acquired by horizontal
243 gene transfer have not been under selective pressure for a sufficiently long period to perform
244 this analysis. In addition, the high rate of codons under negative selection indicate their
245 universal importance in bacterial species. In other words, a molecule under relaxed selective
246 pressure could contribute to the virulence of some populations of the species. However, these
247 features of molecular evolutionary analysis can be advantages when screening for therapeutic
248 target sites or vaccine antigens with a low frequency of missense mutations, which could
249 reduce the virulence or survivability of the pathogen. Evolutionary analysis could also be an
250 effective alternative strategy for overcoming drug resistance through antigen replacement,
251 and could reduce costs associated with drug discovery and development.

252 The *lytA* gene, which was conserved among virtually all pneumococcal strains,
253 showed the highest rates of codons under negative selection, except for *cbpJ* that was only
254 present in some strains. LytA is known to induce pneumococcal-specific autolysis³⁹ and
255 contributes to pneumococcal virulence^{16,40}. Our evolutionary analysis supports previous
256 reports that *lytA* is a suitable genetic marker^{41,42} due to its evolutionary conservation. We also
257 showed that *pspA* and *cbpA* show relatively high rates of codons under positive selection, and
258 both encode polymorphic virulent proteins^{17,19,37} that are candidate vaccine antigens, even

259 though these genes are not universally present within a global serotype 1 collection³⁸. In
260 addition, selective pressure by vaccines can easily cause differentiation or deficiency of these
261 proteins as the corresponding genes contain few codons under negative selection. A
262 multivalent system would be required for vaccines prepared using these antigens.

263 An *in vivo* competition assay in mice indicated that deficiency of *cbpJ* is a
264 disadvantage for pneumococcal survival *in vivo*. On the other hand, co-infection showed a
265 smaller difference in bacterial CFUs between WT and $\Delta cbpJ$ as compared to each single
266 infection. In the single infection of the $\Delta cbpJ$ strain, the bacteria could not be protected by
267 CbpJ. However, in co-infection, the interaction of neutrophils and CbpJ in the WT strain
268 could suppress neutrophil killing activity. In addition, some CbpJ may be released from the
269 WT strain by autolysis. As a result, some of the $\Delta cbpJ$ strain could have been protected
270 similar to the WT strain. Concerning selection, it was previously reported that a single cell
271 bottleneck effect in pneumococcal infection occurs during bloodstream invasion and in
272 transmission between hosts^{43,44}. Our finding also suggests that a bottleneck effect occurs in a
273 limited situation. The difference in bacterial burden of BALF between single and competitive
274 infections suggested a possibility that the bottleneck effect plays a more important role for the
275 selection of *cbpJ*-lacking cells compared to the competition in the lung.

276 In this study, *cbpL* and *cbpJ* were downregulated in the presence of plasma. Although
277 regulation of CBPs is still largely unknown, one possible hypothesis is that the genes are
278 regulated by a pneumococcal two component system (TCS). *S. pneumoniae* interplays with
279 its environment by using 13 TCSs and one orphan response regulator^{45,46}. TCSs typically
280 consist of a membrane-associated sensory protein called a histidine kinase and a cognate
281 cytosolic DNA-binding response regulator, which acts as a transcriptional regulator. Although
282 specific stimuli to histidine kinases still remain unclear, there is a possibility that a histidine
283 kinase sensor protein of the TCSs can respond to some plasma components.

284 Although the difference was not statistically significant, mice intranasally infected
285 with TIGR4 $\Delta cbpL$ strain showed a trend towards improved survival relative to the
286 WT-infected mice. In a previous study, a D39*lux cbpL*-deficient strain showed reduced
287 virulence compared to the WT strain²². Since CbpL sequences in TIGR4 and D39 strains are
288 similar, the discrepancy between the previous study and our findings is likely due to
289 differences in other surface proteins in each strain. For example, the absence of CbpJ, which
290 contributes to the evasion of neutrophil killing, could affect the survivability of D39.

291 Frolet *et al.* reported that both CbpJ and CbpL are considered as possible adhesins
292 because they display interaction with C-reactive protein (CRP), and CRP, elastin, and

293 collagen in solid phase assay, respectively⁴⁷. Meanwhile, Gosink *et al.* showed no significant
294 differences in Detroit nasopharyngeal cells adhesion, rat nasopharynx colonization, and
295 pathogenesis in the sepsis model between the WT and the *cbpJ* mutant strains⁴⁸. Their results
296 are mostly consistent with our data. We also showed that there were no significant differences
297 in the A549 cells adhesion assay and in intravenous infection as a sepsis model. On the other
298 hand, we found a difference in the lethal intranasal mouse infection that is completely
299 different from the non-lethal colonization model. We consider that CbpJ contributes to
300 pneumococcal evasion of host immunity rather than colonization. Concerning CbpL, elastin
301 and collagen are extracellular matrix proteins and binding activity to these proteins could
302 contribute to bacterial adhesion, whereas CRP is found in blood plasma and is used as a
303 marker of inflammation. However, CbpL did not contribute at least to pneumococcal
304 adhesion to A549 cells. There is a discrepancy between protein-protein interactions in the
305 solid phase and host cell-bacteria interactions.

306 Recently, anti-virulence drugs have been developed as an additional strategy to treat
307 or prevent bacterial infections. Drugs targeting bacterial virulence factors are expected to
308 reduce the selective pressure of conventional antibiotics since they would not affect the
309 natural survival of targeted bacteria⁴⁹. Furthermore, the abundance of candidate targets is a

310 major advantage of antivirulence strategies. Effective design of vaccines and antivirulence
311 drugs requires a thorough understanding of virulence factors; combining our evolutionary
312 analysis and traditional molecular microbiological approaches can improve the detection of
313 potential drug targets. In this study, we identified CbpJ as a novel evolutionarily conserved
314 virulence factor. Thus, molecular evolutionary analysis is a powerful system that can reveal
315 the importance of virulence factors in real-world infections and transmission.

316 **Methods**

317 **Phylogenetic and evolutionary analyses**

318 Phylogenetic and evolutionary analyses were performed as described previously^{50,51},
319 with minor modifications. Homologues and orthologues of *cbp* genes were searched using the
320 tBLASTn function of NCBI BLAST. Domain structures of CbpJ and CbpL were searched by
321 MOTIF Search²³ with PROSITE, NCBI-CDD, and P-fam²⁴⁻²⁶. Bacterial ORFs and promoters
322 were predicted by FGENESB (Bacterial Operon and Gene Prediction) and BPROM,
323 respectively⁵². To prevent node density artefacts, sequences with 100% identity were treated
324 as the same sequence in Phylogears2^{53,54}. The sequences were aligned using MAFFT v.7.221
325 with an L-INS-i strategy⁵⁵, and ambiguously aligned regions were removed using Jalview^{56,57}.
326 Calculated orthologous regions were used for further phylogenetic analysis, and edited codon
327 sequences were re-aligned using MAFFT with an L-INS-i strategy. The best-fitting codon
328 evolutionary models for MrBayes and RAxML analyses were determined using Kakusan4⁵⁸.
329 Bayesian Markov chain Monte Carlo analyses were performed with MrBayes v.3.2.5⁵⁹, and 2
330 $\times 10^6$ generations were sampled after confirming that the standard deviation of split
331 frequencies was < 0.01 for up to 8×10^6 generations. To validate phylogenetic inferences,
332 maximum likelihood phylogenetic trees with bootstrap values were generated with RAxML

333 v.8.1.20⁶⁰. Phylogenetic trees were generated using FigTree v.1.4.2⁶¹ based on the calculated
334 data.

335 Evolutionary analyses were performed based on aligned orthologous regions of *cbp*
336 genes and Bayesian phylogenetic trees. Whole-gene non-synonymous/synonymous ratio
337 calculations as well as statistical tests for negative or positive selection of individual codons
338 were performed using the two-rate fixed-effects likelihood function in HyPhy software
339 package⁶².

340

341 **Bacterial strains and construction of mutant strains**

342 *Streptococcus pneumoniae* strains were cultured in Todd-Hewitt broth (BD Biosciences,
343 Franklin Lakes, NJ, USA) supplemented with 0.2% yeast extract (BD Biosciences) (THY
344 medium) at 37°C. For mutant selection and maintenance, spectinomycin (Wako Pure
345 Chemical Industries, Osaka, Japan) was added to the medium at a concentration of 120
346 µg/ml.

347 *S. pneumoniae* TIGR4 isogenic *cbpJ* ($\Delta cbpJ$) and *cbpL* ($\Delta cbpL$) mutant strains were
348 generated as previously described³³. Briefly, the upstream region of *cbpJ* or *cbpL*, an *aad9*
349 cassette, and the downstream region of *cbpJ* or *cbpL* were combined by PCR using the

350 primers shown in Supplementary Table 4. The products were used to construct the mutant
351 strains by double-crossover recombination with the synthesised CSP2⁶³. All mutations were
352 confirmed by PCR amplification of genomic DNA isolated from the mutant strains. For
353 growth measurements, pneumococci were cultured until the optical density at 600 nm
354 (OD₆₀₀) reached 0.4, and the exponential phase cultures of each strain were back-diluted into
355 fresh THY and grown at 37°C. Growth was monitored by measuring the values of OD₆₀₀
356 every 0.5-1 hour. For the following assays, *S. pneumoniae* strains were grown to exponential
357 growth phase (OD₆₀₀ = ~0.4) unless otherwise indicated, and then resuspended in PBS or the
358 appropriate buffer.

359

360 **Preparation of recombinant CbpJ**

361 The *cbpJ* sequence without codons encoding the signal peptide sequence was optimized for *E.*
362 *coli* using GENEius software, and the optimized sequence was synthesized (Eurofins
363 Genomics, Brussel, Belgium). Optimized *cbpJ* and pQE-30 vector (Qiagen, Valencia, CA,
364 USA) were amplified with the specific primers listed in Supplementary Table 5 and
365 PrimeSTAR[®] MAX DNA Polymerase (TaKaRa Bio, Shiga, Japan). The DNA fragments were
366 assembled using the GeneArt[®] Seamless Cloning and Assembly Kit (Thermo Fisher

367 Scientific, Waltham, MA, USA). The constructed plasmid was transformed into *E. coli*
368 XL-10 Gold (Agilent, Santa Clara, CA, USA), and recombinant CbpJ was purified as
369 described previously^{31,33,64-66}.

370

371 **Blood and neutrophil bactericidal assays**

372 A blood bactericidal assay was performed as previously described^{31,33,67}. Mouse blood was
373 obtained via cardiac puncture from healthy female CD-1 mice (Slc:ICR, 6 weeks old; Japan
374 SLC, Hamamatsu, Japan). For human neutrophil isolation, blood was collected via
375 venepuncture from healthy donors after obtaining written, informed consent according to a
376 protocol approved by the institutional review board of Osaka University Graduate School of
377 Dentistry (H26-E43). Neutrophils were isolated from fresh human blood by density gradient
378 centrifugation using Polymorphprep (Alere Technologies, Jena, Germany). Pneumococcal
379 cells grown to the mid-log phase were washed and resuspended in phosphate-buffered saline
380 (PBS). Bacterial cells (1×10^4 CFU/20 μ l) were combined with fresh mouse blood (180 μ l)
381 or human neutrophils (2×10^5 cells/180 μ l) in RPMI 1640 medium, and the mixture was
382 incubated at 37°C with 5% CO₂ for 1, 2, and 3 h. Viable cell counts were determined by
383 seeding diluted samples onto THY blood agar. The percent of the original inoculum was

384 calculated as the number of CFU at the specified time point divided by the number of CFU in
385 the initial inoculum.

386

387 **MIC and MBC assays**

388 Minimum inhibitory concentration (MIC) and minimum bactericidal concentration (MBC)

389 assays were performed as previously described^{51,68}. For MIC and MBC assays, $0.5-1.0 \times 10^4$

390 bacteria were added into THY broth supplemented with 2-fold serial dilutions of penicillin G.

391 Bacterial growth after 24 hours at 37°C in anaerobic conditions was spectrophotometrically

392 measured at OD₆₀₀. We defined the OD₆₀₀ values less than 0.06 as complete inhibition of

393 bacterial growth. To determine MBCs, we inoculated 5 µL of the bacterial cultures onto TS

394 blood agar and incubate them at 37°C in anaerobic conditions. The antimicrobial

395 concentration at which no growth was detectable was defined as the MBC.

396

397 **Mouse infection assays**

398 All mouse experiments were conducted in accordance with animal protocols approved by the

399 Animal Care and Use Committee of Osaka University Graduate School of Dentistry

400 (28-002-0). Female CD-1 mice (Slc:ICR, 6 weeks old) were intranasally infected with $5 \times$

401 10^7 or 2×10^6 CFU of *S. pneumoniae* via the tail vein. Mouse survival was monitored for 14
402 days. At 24 h after intranasal infection, animals were euthanized by lethal intraperitoneal
403 injection of sodium pentobarbital and lung tissue or BALF samples were collected. Bacterial
404 counts in BALF were determined by plating serial dilutions. Lung tissue specimens were
405 fixed with 4% formaldehyde, embedded in paraffin, and cut into sections that were stained
406 with haematoxylin and eosin solution (Applied Medical Research, Osaka, Japan) and
407 visualized with a BZ-X710 microscope (Keyence, Osaka, Japan). For the competition assay,
408 CD-1 mice were intranasally infected with 20 μ L of the mixture of wild-type (1.0×10^7 CFU)
409 and $\Delta cbpJ$ (1.5×10^7 CFU) strains resuspended in PBS, in total, $\sim 2.5 \times 10^7$ CFU. BALF
410 samples were collected at 24 h after infection and bacterial counts in BALF were determined.
411 Total and mutant strain CFUs were determined by serial dilution plating on TS blood agar
412 with or without spectinomycin. The CFU number for the wild-type strain was calculated by
413 subtracting that of the mutant strain from the total CFUs.

414

415 **qPCR**

416 qPCR was performed as previously described^{50,51}, with minor modifications. Primers are
417 listed in Supplementary Table 4. Total RNA of pneumococcal strains grown to the mid-log

418 phase ($OD_{600} = 0.4-0.5$) was isolated with an RNeasy Mini kit (Qiagen) and RQ1 RNase-Free
419 DNase (Promega, Madison, WI, USA), and cDNA was synthesised with SuperScript IV
420 VILO Master Mix (Life Technologies, Carlsbad, CA, USA). qPCR analysis was performed
421 on a StepOnePlus Real-Time PCR system using Power SYBR Green Master PCR mix
422 (Thermo Fisher Scientific). 16S rRNA was used as a normalising control.

423

424 **Statistical analysis**

425 Statistical analysis of *in vitro* and *in vivo* data was performed with Mann-Whitney test,
426 Kruskal-Wallis test with Dunn's multiple comparisons test, Wilcoxon matched-paired signed
427 rank test, and ordinary one-way ANOVA with Tukey's multiple comparisons test. Mouse
428 survival curves were compared with the log-rank test. $P < 0.05$ was considered statistically
429 significant. The tests were performed on Prism v.6.0h or v.7.0d software (GraphPad Inc., La
430 Jolla, CA, USA). All experiments were repeated at least three times. In the evolutionary
431 analyses, $P < 0.1$ was regarded as a significant difference with the HyPhy default setting.

432 **Acknowledgements**

433 This study was supported in part by the Japan Society for the Promotion of Science
434 KAKENHI (grant numbers 15H05012, 16H05847, 16K15787, 17H05103, 17K11666, and
435 17H04369); SECOM Science and Technology Foundation; Takeda Science Foundation; GSK
436 Japan Research Grant; Asahi Glass Foundation; Kurata Memorial Hitachi Science and
437 Technology Foundation; and Kobayashi International Scholarship Foundation. The funders
438 had no role in study design, data collection or analysis, decision to publish, or preparation of
439 the manuscript.

440

441 **Author contributions**

442 M.Y. and S.K. designed the study. M.Y. and Y.Y. performed bioinformatics analyses. K.G.,
443 M.Y., and Y.H. performed the experiments. M.Y., T.S., M.N., and S.K. contributed to the
444 setup of the experimentation. M.Y. wrote the manuscript. G.K., Y.H., Y.Y., T.S., M.N., K.N.,
445 and S.K. contributed to the writing of the manuscript.

446

447 **Competing financial interests statement**

448 The authors declare that they have no competing interests.

449 **References**

- 450 1 O'Neill, J. Tackling drug-resistant infections globally: final report and
451 recommendations. (The Review on Antimicrobial Resistance, 2016).
- 452 2 Paul, S. M. *et al.* How to improve R&D productivity: the pharmaceutical industry's
453 grand challenge. *Nat. Rev. Drug Discov.* **9**, 203-214; doi:10.1038/nrd3078 (2010).
- 454 3 CDC. Antibiotic resistance threats in the United States. (2013).
- 455 4 CDC. *Biggest Threats*,
456 <https://www.cdc.gov/drugresistance/biggest_threats.html> (2017).
- 457 5 WHO. *WHO priority pathogens list for R&D of new antibiotics*,
458 <[http://www.who.int/mediacentre/news/releases/2017/bacteria-antibiotics-n
459 eeded/en/](http://www.who.int/mediacentre/news/releases/2017/bacteria-antibiotics-needed/en/)> (2017).
- 460 6 Richards, V. P. *et al.* Phylogenomics and the dynamic genome evolution of the genus
461 *Streptococcus*. *Genome Biol, Evol.* **6**, 741-753 doi:10.1093/gbe/evu048 (2014).
- 462 7 Kawamura, Y., Hou, X. G., Sultana, F., Miura, H. & Ezaki, T. Determination of 16S
463 rRNA sequences of *Streptococcus mitis* and *Streptococcus gordonii* and phylogenetic
464 relationships among members of the genus *Streptococcus*. *Int. J. Syst. Bacteriol.* **45**,
465 406-408; doi:10.1099/00207713-45-2-406 (1995).
- 466 8 Walker, C. L. *et al.* Global burden of childhood pneumonia and diarrhoea. *Lancet* **381**,
467 1405-1416; doi:10.1016/S0140-6736(13)60222-6 (2013).
- 468 9 Castelblanco, R. L., Lee, M. & Hasbun, R. Epidemiology of bacterial meningitis in
469 the USA from 1997 to 2010: a population-based observational study. *Lancet Infect.
470 Dis.* **14**, 813-819; doi:10.1016/S1473-3099(14)70805-9 (2014).
- 471 10 GBD 2015 LRI Collaborators. Estimates of the global, regional, and national
472 morbidity, mortality, and aetiologies of lower respiratory tract infections in 195
473 countries: a systematic analysis for the Global Burden of Disease Study 2015. *Lancet
474 Infect. Dis.* **17**, 1133-1161; doi:10.1016/S1473-3099(17)30396-1 (2017).
- 475 11 Golubchik, T. *et al.* Pneumococcal genome sequencing tracks a vaccine escape variant
476 formed through a multi-fragment recombination event. *Nat. Genet.* **44**, 352-355;
477 doi:10.1038/ng.1072 (2012).
- 478 12 Flasche, S. *et al.* Effect of pneumococcal conjugate vaccination on serotype-specific
479 carriage and invasive disease in England: a cross-sectional study. *PLoS Med.* **8**,
480 e1001017; doi:10.1371/journal.pmed.1001017 (2011).
- 481 13 Brockhurst, M. A. *et al.* Running with the Red Queen: the role of biotic conflicts in
482 evolution. *Proc. Biol. Sci.* **281**; doi:10.1098/rspb.2014.1382 (2014).
- 483 14 Sironi, M., Cagliani, R., Forni, D. & Clerici, M. Evolutionary insights into

- 484 host-pathogen interactions from mammalian sequence data. *Nat. Rev. Genet.* **16**,
485 224-236; doi:10.1038/nrg3905 (2015).
- 486 15 Jordan, I. K., Rogozin, I. B., Wolf, Y. I. & Koonin, E. V. Essential genes are more
487 evolutionarily conserved than are nonessential genes in bacteria. *Genome Res.* **12**,
488 962-968; doi:10.1101/gr.87702 (2002).
- 489 16 Berry, A. M., Lock, R. A., Hansman, D. & Paton, J. C. Contribution of autolysin to
490 virulence of *Streptococcus pneumoniae*. *Infect. Immun.* **57**, 2324-2330 (1989).
- 491 17 Hakenbeck, R., Madhour, A., Denapaite, D. & Bruckner, R. Versatility of choline
492 metabolism and choline-binding proteins in *Streptococcus pneumoniae* and
493 commensal streptococci. *FEMS Microbiol. Rev* **33**, 572-586 (2009).
- 494 18 Maestro, B. & Sanz, J. M. Choline binding proteins from *Streptococcus pneumoniae*:
495 a dual role as enzybiotics and targets for the design of new antimicrobials. *Antibiotics*
496 (*Basel*) **5**; doi:10.3390/antibiotics5020021 (2016).
- 497 19 Hollingshead, S. K. *et al.* Pneumococcal surface protein A (PspA) family distribution
498 among clinical isolates from adults over 50 years of age collected in seven countries.
499 *J Med. Microbiol.* **55**, 215-221; doi:10.1099/jmm.0.46268-0 (2006).
- 500 20 Ren, B. *et al.* The virulence function of *Streptococcus pneumoniae* surface protein A
501 involves inhibition of complement activation and impairment of complement
502 receptor-mediated protection. *J. Immunol.* **173**, 7506-7512 (2004).
- 503 21 Dave, S., Carmicle, S., Hammerschmidt, S., Pangburn, M. K. & McDaniel, L. S. Dual
504 roles of PspC, a surface protein of *Streptococcus pneumoniae*, in binding human
505 secretory IgA and factor H. *J. Immunol.* **173**, 471-477 (2004).
- 506 22 Gutierrez-Fernandez, J. *et al.* Modular architecture and unique teichoic acid
507 recognition features of choline-binding protein L (CbpL) contributing to
508 pneumococcal pathogenesis. *Sci. Rep.* **6**, 38094; doi:10.1038/srep38094 (2016).
- 509 23 Kanehisa, M. & Goto, S. KEGG: Kyoto encyclopedia of genes and genomes. *Nucleic*
510 *Acids Res.* **28**, 27-30 (2000).
- 511 24 Sigrist, C. J. *et al.* New and continuing developments at PROSITE. *Nucleic Acids Res.*
512 **41**, D344-347; doi:10.1093/nar/gks1067 (2013).
- 513 25 Marchler-Bauer, A. *et al.* CDD: conserved domains and protein three-dimensional
514 structure. *Nucleic Acids Res.* **41**, D348-352; doi:10.1093/nar/gks1243 (2013).
- 515 26 Finn, R. D. *et al.* Pfam: the protein families database. *Nucleic Acids Res.* **42**,
516 D222-230; doi:10.1093/nar/gkt1223 (2014).
- 517 27 Fumagalli, M. & Sironi, M. Human genome variability, natural selection and
518 infectious diseases. *Curr. Opin. Immunol.* **30**, 9-16; doi:10.1016/j.coi.2014.05.001

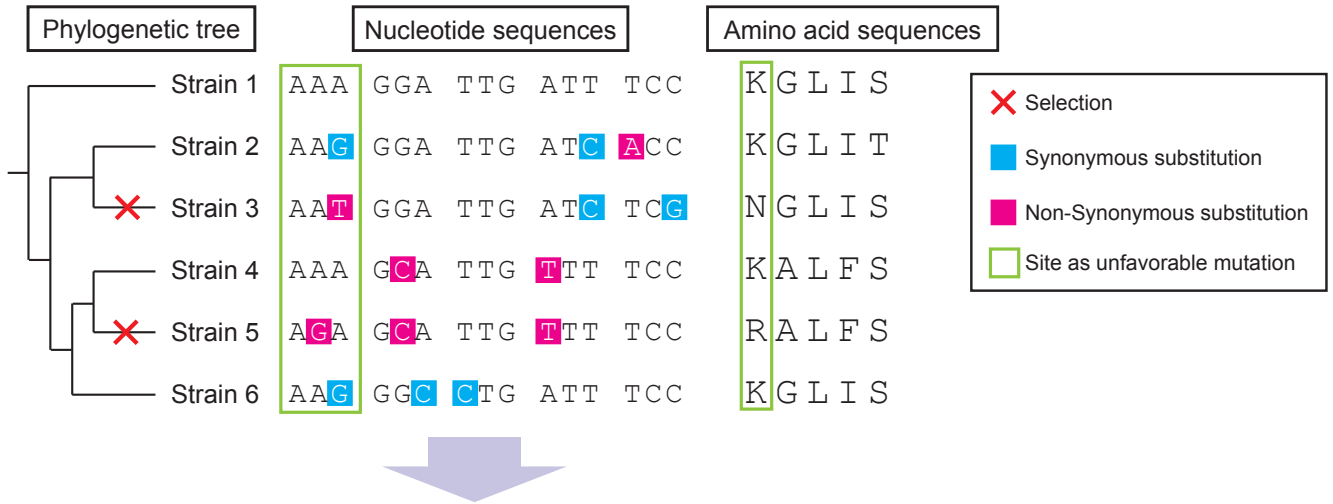
- 519 (2014).
- 520 28 Karlsson, E. K., Kwiatkowski, D. P. & Sabeti, P. C. Natural selection and infectious
521 disease in human populations. *Nat. Rev. Genet.* **15**, 379-393; doi:10.1038/nrg3734
522 (2014).
- 523 29 Siddle, K. J. & Quintana-Murci, L. The Red Queen's long race: human adaptation to
524 pathogen pressure. *Curr. Opin. Genet. Dev.* **29**, 31-38; doi:10.1016/j.gde.2014.07.004
525 (2014).
- 526 30 Terao, Y. *et al.* Group A streptococcal cysteine protease degrades C3 (C3b) and
527 contributes to evasion of innate immunity. *J. Biol. Chem.* **283**, 6253-6260;
528 doi:10.1074/jbc.M704821200 (2008).
- 529 31 Yamaguchi, M., Terao, Y., Mori, Y., Hamada, S. & Kawabata, S. PfbA, a novel
530 plasmin- and fibronectin-binding protein of *Streptococcus pneumoniae*, contributes to
531 fibronectin-dependent adhesion and antiphagocytosis. *J. Biol. Chem.* **283**,
532 36272-36279; doi:10.1074/jbc.M807087200 (2008).
- 533 32 Sumitomo, T. *et al.* Streptolysin S contributes to group A streptococcal translocation
534 across an epithelial barrier. *J. Biol. Chem.* **286**, 2750-2761;
535 doi:10.1074/jbc.M110.171504 (2011).
- 536 33 Mori, Y. *et al.* alpha-Enolase of *Streptococcus pneumoniae* induces formation of
537 neutrophil extracellular traps. *J. Biol. Chem.* **287**, 10472-10481;
538 doi:10.1074/jbc.M111.280321 (2012).
- 539 34 Yamaguchi, M. *et al.* *Streptococcus pneumoniae* invades erythrocytes and utilizes
540 them to evade human innate immunity. *PLoS One* **8**, e77282;
541 doi:10.1371/journal.pone.0077282 (2013).
- 542 35 Gallagher, M. D. & Chen-Plotkin, A. S. The post-GWAS era: from association to
543 function. *Am. J. Hum. Genet.* **102**, 717-730; doi:10.1016/j.ajhg.2018.04.002 (2018).
- 544 36 Marigorta, U. M., Rodriguez, J. A., Gibson, G. & Navarro, A. Replicability and
545 prediction: lessons and challenges from GWAS. *Trends Genet.* **34**, 504-517;
546 doi:10.1016/j.tig.2018.03.005 (2018).
- 547 37 Brooks-Walter, A., Briles, D. E. & Hollingshead, S. K. The *pspC* gene of
548 *Streptococcus pneumoniae* encodes a polymorphic protein, PspC, which elicits
549 cross-reactive antibodies to PspA and provides immunity to pneumococcal bacteremia.
550 *Infect. Immun.* **67**, 6533-6542 (1999).
- 551 38 Cornick, J. E. *et al.* The global distribution and diversity of protein vaccine candidate
552 antigens in the highly virulent *Streptococcus pneumoniae* serotype 1. *Vaccine* **35**,
553 972-980; doi:10.1016/j.vaccine.2016.12.037 (2017).

- 554 39 Mosser, J. L. & Tomasz, A. Choline-containing teichoic acid as a structural
555 component of pneumococcal cell wall and its role in sensitivity to lysis by an
556 autolytic enzyme. *J. Biol. Chem.* **245**, 287-298 (1970).
- 557 40 Orihuela, C. J., Gao, G., Francis, K. P., Yu, J. & Tuomanen, E. I. Tissue-specific
558 contributions of pneumococcal virulence factors to pathogenesis. *J. Infect. Dis.* **190**,
559 1661-1669; doi:10.1086/424596 (2004).
- 560 41 Carvalho Mda, G. *et al.* Evaluation and improvement of real-time PCR assays
561 targeting *lytA*, *ply*, and *psaA* genes for detection of pneumococcal DNA. *J. Clin.*
562 *Microbiol.* **45**, 2460-2466; doi:10.1128/JCM.02498-06 (2007).
- 563 42 Saukkoriipi, A. *et al.* *lytA* Quantitative PCR on sputum and nasopharyngeal swab
564 samples for detection of pneumococcal pneumonia among the elderly. *J. Clin.*
565 *Microbiol.* **56**, e01231-012317; doi:10.1128/JCM.01231-17 (2018).
- 566 43 Gerlini, A. *et al.* The role of host and microbial factors in the pathogenesis of
567 pneumococcal bacteraemia arising from a single bacterial cell bottleneck. *PLoS*
568 *Pathog.* **10**, e1004026; doi:10.1371/journal.ppat.1004026 (2014).
- 569 44 Kono, M. *et al.* Single cell bottlenecks in the pathogenesis of *Streptococcus*
570 *pneumoniae*. *PLoS Pathog.* **12**, e1005887; doi:10.1371/journal.ppat.1005887 (2016).
- 571 45 Lange, R. *et al.* Domain organization and molecular characterization of 13
572 two-component systems identified by genome sequencing of *Streptococcus*
573 *pneumoniae*. *Gene* **237**, 223-234 (1999).
- 574 46 Throup, J. P. *et al.* A genomic analysis of two-component signal transduction in
575 *Streptococcus pneumoniae*. *Mol. Microbiol.* **35**, 566-576 (2000).
- 576 47 Frolet, C. *et al.* New adhesin functions of surface-exposed pneumococcal proteins.
577 *BMC Microbiol.* **10**, 190; doi:10.1186/1471-2180-10-190 (2010).
- 578 48 Gosink, K. K., Mann, E. R., Guglielmo, C., Tuomanen, E. I. & Masure, H. R. Role of
579 novel choline binding proteins in virulence of *Streptococcus pneumoniae*. *Infect.*
580 *Immun.* **68**, 5690-5695 (2000).
- 581 49 Dickey, S. W., Cheung, G. Y. C. & Otto, M. Different drugs for bad bugs:
582 antivirulence strategies in the age of antibiotic resistance. *Nat. Rev. Drug Discov.* **16**,
583 457-471; doi:10.1038/nrd.2017.23 (2017).
- 584 50 Yamaguchi, M. *et al.* Evolutionary inactivation of a sialidase in group B
585 *Streptococcus*. *Sci. Rep.* **6**, 28852l doi:10.1038/srep28852 (2016).
- 586 51 Yamaguchi, M. *et al.* Zinc metalloproteinase ZmpC suppresses experimental
587 pneumococcal meningitis by inhibiting bacterial invasion of central nervous systems.
588 *Virulence* **8**, 1516-1524; doi:10.1080/21505594.2017.1328333 (2017).

- 589 52 Solovyev, V. & Salamov, A. in *Metagenomics and its Applications in Agriculture, Biomedicine and Environmental Studies* (ed. Li, W.R.) Ch. 4, 61-78 (Nova Science Publishers, 2011).
- 590
- 591
- 592 53 Tanabe, A. S. *Phylogears2 ver. 2.0*, <<http://www.fifthdimension.jp/>> (2008).
- 593 54 Venditti, C., Meade, A. & Pagel, M. Detecting the node-density artifact in phylogeny reconstruction. *Syst. Biol.* **55**, 637-643 (2006).
- 594
- 595 55 Katoh, K. & Standley, D. M. MAFFT multiple sequence alignment software version 7: improvements in performance and usability. *Mol. Biol. Evol.* **30**, 772-780; doi:10.1093/molbev/mst010 (2013).
- 596
- 597
- 598 56 Waterhouse, A. M., Procter, J. B., Martin, D. M., Clamp, M. & Barton, G. J. Jalview Version 2--a multiple sequence alignment editor and analysis workbench. *Bioinformatics* **25**, 1189-1191; doi:10.1093/bioinformatics/btp033 (2009).
- 599
- 600
- 601 57 Talavera, G. & Castresana, J. Improvement of phylogenies after removing divergent and ambiguously aligned blocks from protein sequence alignments. *Syst. Biol.* **56**,
- 602
- 603 564-577; doi:10.1080/10635150701472164 (2007).
- 604 58 Tanabe, A. S. Kakusan4 and Aminosan: two programs for comparing nonpartitioned, proportional and separate models for combined molecular phylogenetic analyses of multilocus sequence data. *Mol. Ecol. Resour.* **11**, 914-921; doi:10.1111/j.1755-0998.2011.03021.x (2011).
- 605
- 606
- 607
- 608 59 Ronquist, F. *et al.* MrBayes 3.2: efficient Bayesian phylogenetic inference and model choice across a large model space. *Syst. Biol.* **61**, 539-542; doi:10.1093/sysbio/sys029 (2012).
- 609
- 610
- 611 60 Stamatakis, A. RAxML version 8: a tool for phylogenetic analysis and post-analysis of large phylogenies. *Bioinformatics* **30**, 1312-1313; doi:10.1093/bioinformatics/btu033 (2014).
- 612
- 613
- 614 61 Rambaut, A. *FigTree ver.1.4.2*, <<http://tree.bio.ed.ac.uk/software/figtree/>> (2014).
- 615
- 616 62 Pond, S. L., Frost, S. D. & Muse, S. V. HyPhy: hypothesis testing using phylogenies. *Bioinformatics* **21**, 676-679; doi:10.1093/bioinformatics/bti079 (2005).
- 617
- 618 63 Bricker, A. L. & Camilli, A. Transformation of a type 4 encapsulated strain of *Streptococcus pneumoniae*. *FEMS Microbiol. Lett.* **172**, 131-135 (1999).
- 619
- 620 64 Beulin, D. S., Yamaguchi, M., Kawabata, S. & Ponnuraj, K. Crystal structure of PfbA, a surface adhesin of *Streptococcus pneumoniae*, provides hints into its interaction with fibronectin. *Int. J. Biol. Macromol.* **64**, 168-173; doi:10.1016/j.ijbiomac.2013.11.035 (2014).
- 621
- 622
- 623

- 624 65 Beulin, D. S. J. *et al.* *Streptococcus pneumoniae* surface protein PfbA is a versatile
625 multidomain and multiligand-binding adhesin employing different binding
626 mechanisms. *FEBS J.* **284**, 3404-3421; doi:10.1111/febs.14200 (2017).
- 627 66 Radhakrishnan, D., Yamaguchi, M., Kawabata, S. & Ponnuraj, K. *Streptococcus*
628 *pneumoniae* surface adhesin PfbA and its interaction with erythrocytes and
629 hemoglobin. *Int. J. Biol. Macromol.* **120**, 135-143;
630 doi:10.1016/j.ijbiomac.2018.08.080 (2018).
- 631 67 Yamaguchi, M. *et al.* Role of *Streptococcus sanguinis* sortase A in bacterial
632 colonization. *Microbes Infect.* **8**, 2791-2796; doi:10.1016/j.micinf.2006.08.010
633 (2006).
- 634 68 Hirose, Y. *et al.* Competence-induced protein Ccs4 facilitates pneumococcal invasion
635 into brain tissue and virulence in meningitis. *Virulence* **9**, 1576-1587;
636 doi:10.1080/21505594.2018.1526530 (2018).
- 637
638

A. Phylogenetic relationship before natural selection



B. Real population resulting from natural selection



Figure 1. Scheme for intra-species molecular evolutionary analysis. **A.** Random genetic drift induces synonymous and non-synonymous mutations with equal probability. However, non-synonymous mutations in the essential region cause host selection. **B.** As a result of natural selection, synonymous substitutions are concentrated in important genes. Phylogenetic and molecular evolutionary analyses can detect significant accumulation of synonymous substitutions in codons of host proteins. Codon-based analysis yields much more information than nucleotide- or amino acid-based analyses.

A

Serotype	4	1	1	1	1	2	N.T.	3	3	3	3	3	3	3	5	6B	11A	14	14	19A	19A	19F	19F	19F	19F	23F	N.T.		
Strain	TIGR4	P1031	INV104	gamPNI0373	NCTC7465	D39	R6	SPNA45	OXC141	SPN034156	SPN034183	SPN994038	SPN994039	A66	70585	670-6B	AP200	CGSP14	INV200	Hungary19A-6	TCH8431/19A	JJA	Taiwan19F-14	G54	ST1556	A026	ATCC 700669	NT_110_58	
Gene	TIGR4	P1031	INV104	gamPNI0373	NCTC7465	D39	R6	SPNA45	OXC141	SPN034156	SPN034183	SPN994038	SPN994039	A66	70585	670-6B	AP200	CGSP14	INV200	Hungary19A-6	TCH8431/19A	JJA	Taiwan19F-14	G54	ST1556	A026	ATCC 700669	NT_110_58	
<i>cbpA</i>																													
<i>cbpC</i>																													
<i>cbpD</i>																													
<i>cbpE</i>																													
<i>cbpF</i>								*																					
<i>cbpG</i>																													
<i>cbpI</i>																													
<i>cbpJ</i>								*																					
<i>cbpK</i>																													
<i>cbpL</i>																													
<i>cbpM</i>																													
<i>lytA</i>																													
<i>lytB</i>																													
<i>lytC</i>																													
<i>pcpA</i>																													
<i>pspA</i>																													

B

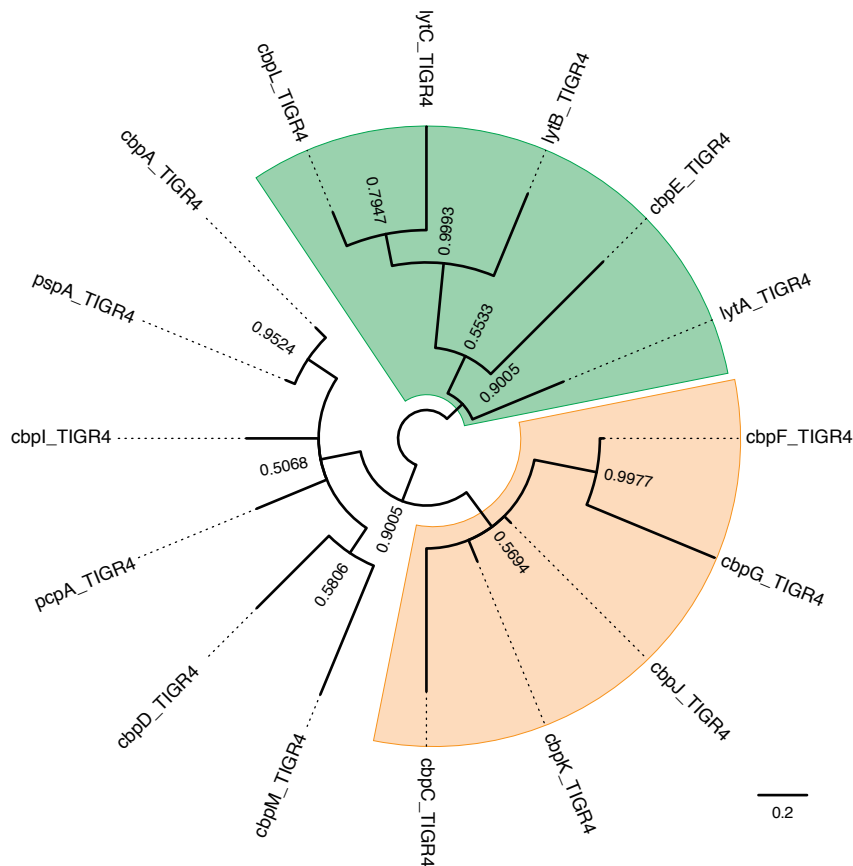
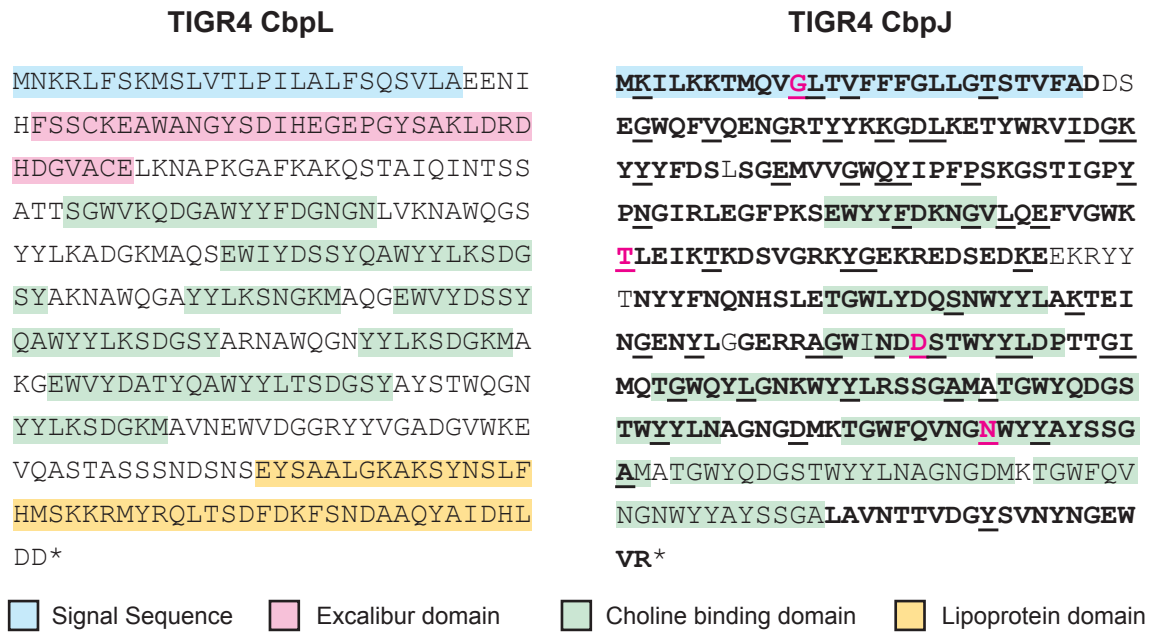


Figure 2. Yamaguchi *et al.*

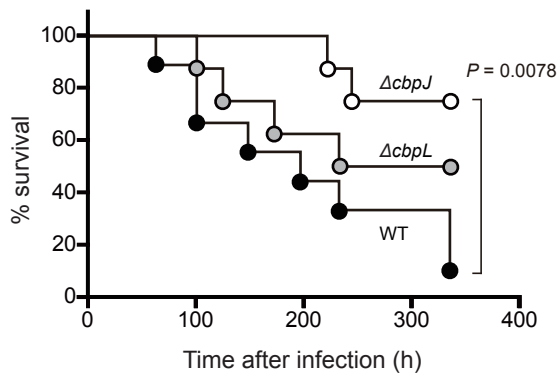
Figure 2. Distribution of *cbp* genes and phylogenetic relationship in TIGR4. **A.** Distribution of genes encoding CBPs among pneumococcal strains. The gene locus tag numbers are shown in Supplementary Table 1. Blue, yellow, and gray show the presence, pseudogenisation, and absence of genes, respectively. *These genes are annotated as one gene, but our bioinformatic analysis indicates that they are independent genes. **B.** Nucleotide-based Bayesian phylogenetic tree of *cbp* genes of *S. pneumoniae* strain TIGR4. The tree is unrooted and posterior probabilities are shown near the nodes. The scale bar indicates nucleotide substitutions per site.

Figure 3: Phylogenetic analyses of *cbp* genes with high similarity. A, B. Nucleotide-based Bayesian phylogenetic tree of the *lytA*, *lytB*, *lytC*, *cbpE*, and *cbpL* genes (A) and the *cbpF*, *cbpG*, *cbpJ*, and *cbpK* genes (B) in *S. pneumoniae*. The trees are unrooted although they are presented as midpoint-rooted for clarity. Strains with identical sequences are listed on the same branch. Posterior probabilities are shown near the nodes. The scale bar indicates nucleotide substitutions per site.

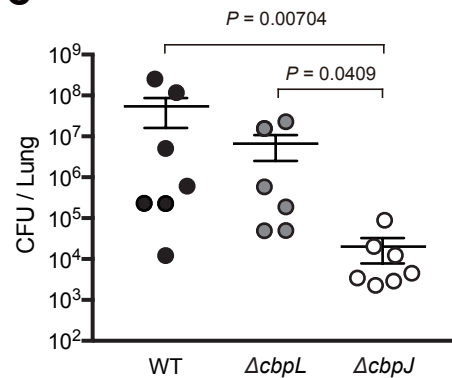
A



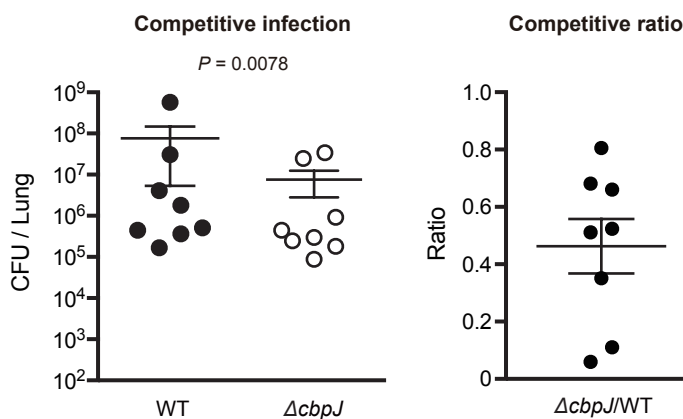
B



C



D



E

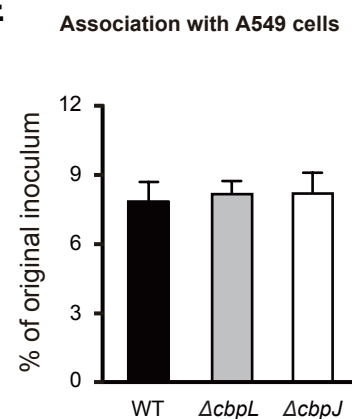
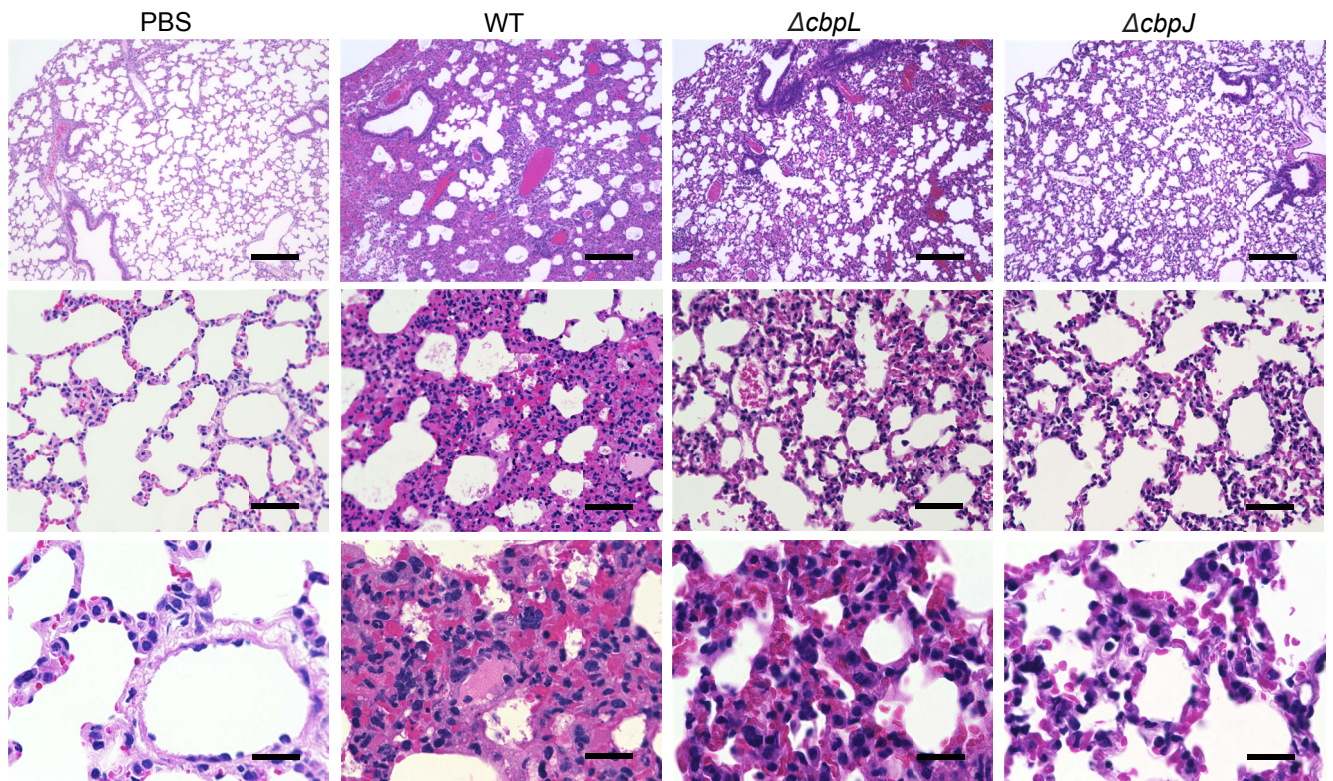


Figure 4. Yamaguchi *et al.*

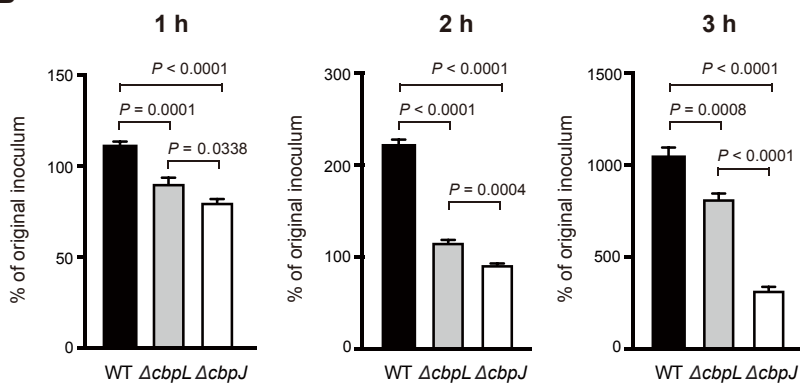
Figure 4: Deficiency of *cbpJ* decreased pneumococcal virulence in mouse pneumonia model.

A. Amino acid sequences and domain structures of CbpL and CbpJ in strain TIGR4. Bold, black underlined, and magenta underlined characters represent comparable codons and those under purifying or positive selection, respectively. **B.** Mouse pneumonia model. Mice were intranasally infected with 5×10^7 CFU of *S. pneumoniae* TIGR4 WT, $\Delta cbpL$, or $\Delta cbpJ$ strains, and survival was monitored for 14 days. **C.** Pneumococcal CFU in BALF collected at 24 h after intranasal infection. The difference between groups was analysed using the Kruskal-Wallis test with Dunn' s multiple comparisons test. **D.** *S. pneumoniae* TIGR4 WT and $\Delta cbpJ$ strains were examined for their competitive infection activities. BALF was collected at 24 h after intranasal infection. The difference between groups was analysed with the Wilcoxon matched-paired signed rank test. **E.** *S. pneumoniae* TIGR4 WT, $\Delta cbpL$, and $\Delta cbpJ$ strains were examined for their ability to associate with A549 cells. Differences between groups were analysed using ordinary one-way ANOVA with Tukey' s multiple comparisons test. Data are presented as the mean of six samples with standard error (C, D, E).

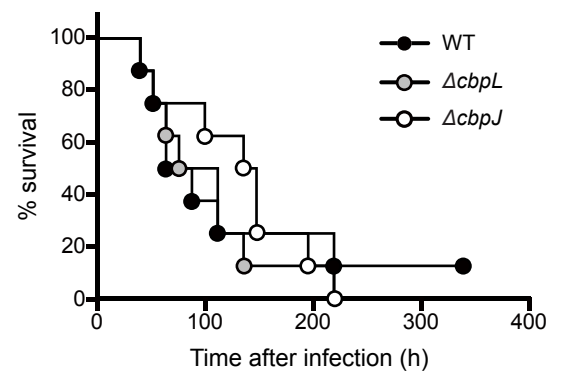
A



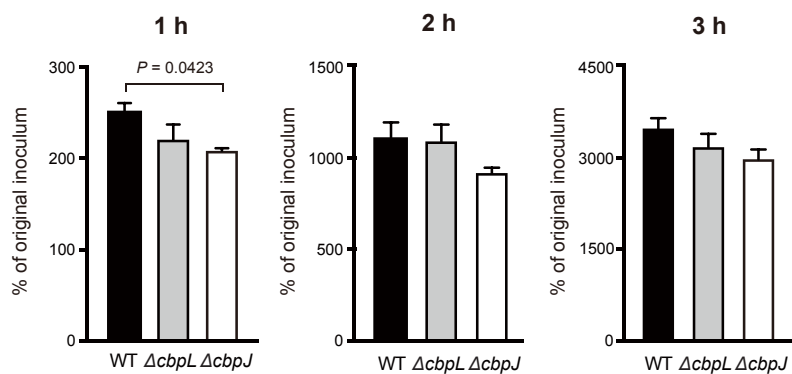
B



C



D



E

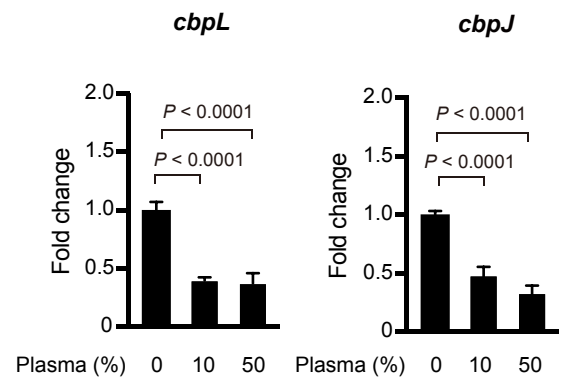


Figure 5. Yamaguchi *et al.*

Figure 5: *cbpJ* and *cbpL* are downregulated in the presence of plasma, and do not affect pneumococcal survival in mouse blood. **A.** Haematoxylin and eosin staining of infected mouse lung tissue collected 24 h after intranasal infection with 5×10^7 CFU of *S. pneumoniae* TIGR4 WT, $\Delta cbpL$, or $\Delta cbpJ$ strains. Scale bars, 200 μm (upper panels), 50 μm (middle panels), and 20 μm (lower panels). **B.** Growth of pneumococcal strains in the presence of human neutrophils. Bacterial cells were incubated with neutrophils for 1, 2, and 3 h at 37°C and 5% CO_2 , then serially diluted and plated on TS blood agar. The number of CFUs was determined following incubation. Growth index was calculated by dividing CFU after incubation by the CFU of the original inoculum. Data are presented as the mean of six samples with standard error. **C.** Mouse sepsis model. Mice were intravenously infected with 2×10^6 CFU of *S. pneumoniae* TIGR4 WT, $\Delta cbpL$, or $\Delta cbpJ$, and survival was monitored for 14 days. Differences between infected mouse groups were analysed with the log-rank test. **D.** Growth of pneumococcal strains in mouse blood. Bacterial cells were incubated in blood for 1, 2, and 3 h at 37°C and 5% CO_2 . Data are presented as the mean of six samples with standard error. **E.** Fold transcript levels of *cbpL* and *cbpJ* in TIGR4 WT *S. pneumoniae* cells in the presence or absence of human plasma. 16S rRNA was used as an internal standard. Data were pooled and normalised from three independent experiments, each performed in quadruplicate.

639 **Table 1.** Evolutionary analyses of genes encoding choline-binding proteins*

Genes	Number of sequences ¹	dN/dS	Coverage of comparable codons relative to whole protein in TIGR4	Codons evolving under positive selection	Codons evolving under purifying selection	% Of codons under purifying selection relative to total codons
<i>cbpA</i>	19	0.864	22.334% (155/694)	3.226% (5/155)	7.742% (12/155)	1.729%
<i>cbpC</i>	13	–	0% (0/93)	–	–	0.000%
<i>cbpD</i>	19	0.359	75.278% (338/449)	0.296% (1/338)	3.550% (12/338)	2.672%
<i>cbpE</i>	18	0.325	99.363% (624/628)	0.160% (1/624)	4.968% (31/624)	4.936%
<i>cbpF</i>	19	0.395	60.411% (206/341)	0.485% (1/206)	3.398% (7/206)	2.053%
<i>cbpG</i>	21	–	0% (0/286)	–	–	0.000%
<i>cbpI</i>	2	–	–	–	–	–
<i>cbpJ</i>	15	0.346	84.084% (280/333)	1.429% (4/280)	18.571% (52/280)	15.616%
<i>cbpK</i>	11	0.353	85.630% (292/341)	0.342% (1/292)	3.082% (9/292)	2.639%
<i>cbpL</i>	20	–	0% (0/333)	–	–	0.000%
<i>cbpM</i>	10	0.642	98.462% (128/130) ²	0% (0/128)	0% (0/128)	0.000%
<i>lytA</i>	14	0.141	80.564% (257/319)	0% (0/257)	17.121% (44/257)	13.793%
<i>lytB</i>	22	0.185	92.868% (612/659)	0% (0/612)	4.739% (29/612)	4.401%
<i>lytC</i>	23	0.400	19.348% (95/491)	0% (0/95)	5.263% (5/95)	1.018%
<i>pcpA</i>	18	0.261	77.010% (479/622)	0% (0/479)	0.418% (2/479)	0.322%
<i>pspA</i>	24	0.857	19.060% (142/745)	6.338% (9/142)	12.676% (18/142)	2.416%

640 ¹Sequences with 100% identity were treated as the same sequence; ²compared to D39.

641 *Evolutionary analysis was performed by Bayesian inference of aligned *cbp* sequences from complete genomes of *S. pneumoniae* with the two-rate fixed-effects
642 likelihood function in HyPhy software package. dN/dS is the ratio of non-synonymous to synonymous changes in overall analysed genes. Individual codons with a
643 statistically significant signature were also calculated and are expressed as a percentage of the total number of codons included in the analysis.